Engineering Conferences International

ECI Digital Archives

The 14th International Conference on Fluidization – From Fundamentals to Products

Refereed Proceedings

1-1-2013

Design of a Statistical Strategy to the Control of a Fluidized Bed Equipped with a Rotating Distributor

J. Gómez-Hernández
Carlos III University of Madrid, Spain

A. Soria-Verdugo
Carlos III University of Madrid, Spain

J. Villa Briongos
Carlos III University of Madrid, Spain

D. Santana
Carlos III University of Madrid, Spain

Follow this and additional works at: http://dc.engconfintl.org/fluidization_xiv

 Part of the Chemical Engineering Commons

Recommended Citation

J. Gómez-Hernández, A. Soria-Verdugo, J. Villa Briongos, and D. Santana, "Design of a Statistical Strategy to the Control of a Fluidized Bed Equipped with a Rotating Distributor" in "The 14th International Conference on Fluidization – From Fundamentals to Products", Eds, ECI Symposium Series, Volume (2013). http://dc.engconfintl.org/fluidization_xiv/79

This Article is brought to you for free and open access by the Refereed Proceedings at ECI Digital Archives. It has been accepted for inclusion in The 14th International Conference on Fluidization – From Fundamentals to Products by an authorized administrator of ECI Digital Archives. For more information, please contact franco@bepress.com.

DESIGN OF A STATISTICAL STRATEGY TO THE CONTROL OF A FLUIDIZED BED EQUIPPED WITH A ROTATING DISTRIBUTOR

J. Gómez-Hernández [a]*, A. Soria-Verdugo, J. Villa Briongos, D. Santana
[a]Carlos III University of Madrid; Dept. of Thermal and Fluid Mechannics
Avda. Universidad 30, 28911 Leganés, Madrid, Spain
*T: 0034-916248371; F: 0034-916249430; E: jegomez@ing.uc3m.es

ABSTRACT

The present work proposes the use of the so-called “moving mean control charts” for the continuous monitoring of the fluidized bed. A rotating distributor was used as a counteracting measurement against the defluidization phenomena. The results showed the utility of the proposed strategy to identify the defluidization and recuperation processes.

INTRODUCTION

Bubbling fluidized beds are used for a wide variety of industrial processes, such as the chemical, food, and pharmaceutical industries. For any process, it is desirable to be able to specify the level at which it is operating, and therefore, it is customary for the implementation of a monitoring and control system that can ensure the operation at a certain level of performance. All these operations require the measurement of the fluidization state and the possibility to modify the operational conditions to exert the control of the process. The development of online control strategies using pressure fluctuation signals is still incipient, due to noisy pressure time series, which are difficult to monitor (1). Statistical process control (SPC) methods have been widely used in industry processes for fault detection (2). Such a strategy is based on the data representation in control charts, which are used to analyze the variability of processes, helping to find the causes of changes and monitor performance.

The present work proposes a methodology to design the control scheme for a general fluidized bed process. Such a control strategy approach is based on the implementation and use of the moving mean control charts for the pressure fluctuations measured in the plenum chamber. Therefore, the control strategy results should identify the out of the control state and will help in the identification of the uncontrolled states causes. To that end, the proposed control strategy is designed according to the SPC principles, and the obtained control charts are analyzed for the defluidization of the bed caused by the agglomeration formation. A rotating distributor will be used as a counteracting measurement against this defluidization phenomenon.

EXPERIMENTAL SETUP

The experiments were carried out in a lab-scale cylindrical Bubbling Fluidized Bed (BFB), equipped with an electrical motor in order to produce a rotation of the distributor. The cylindrical vessel has an inner diameter, D, of 0.192 m, and a height of 1 m. The packed bed height, h_b, is fixed to a value of $0.75 \cdot D$. The rotating distributor was a perforated plate with an open area of 3% and the holes were laid out in a triangular mesh with a pitch of 11 mm. During the experiments, it can be discriminated between the rotational distributor case, with an angular velocity of 100

rpm, and the static distributor case, without any rotation. A schematic of the setup is shown in Fig. 1. The bed material was silica sand particles, classified as Group B according to Geldart's classification (3). The particle density was measured to be 2,645.5 kg/m^3 with a standard deviation of 2.5 kg/m^3, and a mean diameter of 683 μm.

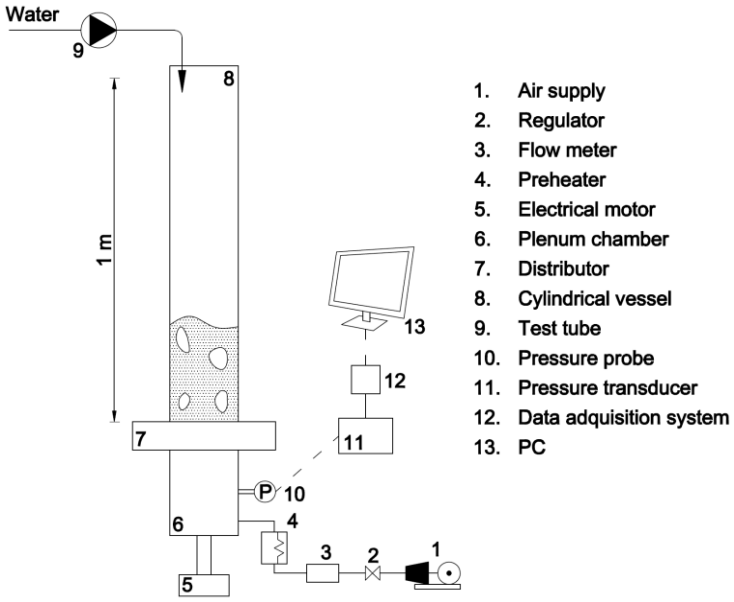

Fig. 1: Schematic diagram of the experimental fluidized bed.

The measurement system consists of one pressure probe with 4 mm of internal diameter and a length of 0.10 m. These dimensions guarantee an undisturbed transfer of the pressure signal and a reliable measurement (4-5). Piezoelectric pressure sensors, Kistler type 7261, were connected to the probes to measure the differential pressure fluctuations. The measurements from the Kistler 5015 sensors were amplified using a Kistler amplifier type 50515. The signal was stored in a PC using a National Instruments data acquisition system type 9234 working at a sampling frequency of 400 Hz.

METHODOLOGY

During the tests the relative fluidization velocity was set to a value of U/U_{mf} = 1.6, and the fluidized bed was operated at a constant inlet temperature of 30º C. These settings will be referred to as *nominal conditions* and will define the steady state operation of the lab-scale fluidized bed. The experiments were carried out for shallow beds with h_b/D = 0.75. The minimum fluidization velocity was measured to be $U_{mf,s}$ = 0.33 m/s and $U_{mf,r}$ = 0.31 m/s for the static and rotating distributor respectively (6).

All the experiments started with the fluidized bed operating at nominal conditions, with no rotation of the distributor and no agglomerates present. The agglomerates were formed due to the punctual injection of water. To start the agglomeration process, 150 ml of water were instantaneously injected using a test tube to spill the water on the surface of the bed from 1 m over the distributor and perpendicular to it. After the defluidization of the bed, the water injection was stopped and the rotating

distributor was switched on as a counteracting measure against the agglomeration of the bed, trying to recover the fluidization quality of the controlled state of the bed.

METHODS OF ANALYSIS

According to the basic strategy of control proposed in this work, the variables of control were obtained by analyzing the pressure fluctuations with linear methods. The analysis covered both the time and the frequency domains giving a complete outline of the fluidization behavior.

Time domain analysis

The standard deviation of the pressure signal was employed to analyze the behavior of the bed in the time domain. As stated by van Ommen et al. (7) the variation in the standard deviation can be used to identify the regime change and the defluidization of the bed, as can be seen in Fig. 2-a.

The average cycle time, *tav*, was also calculated. This parameter can be defined as twice the total measurement time divided by the number of crossings with the average value (8). As expected, the average cycle time detects the transition between the defluidized and the fluidized regimes, Fig. 2-a.

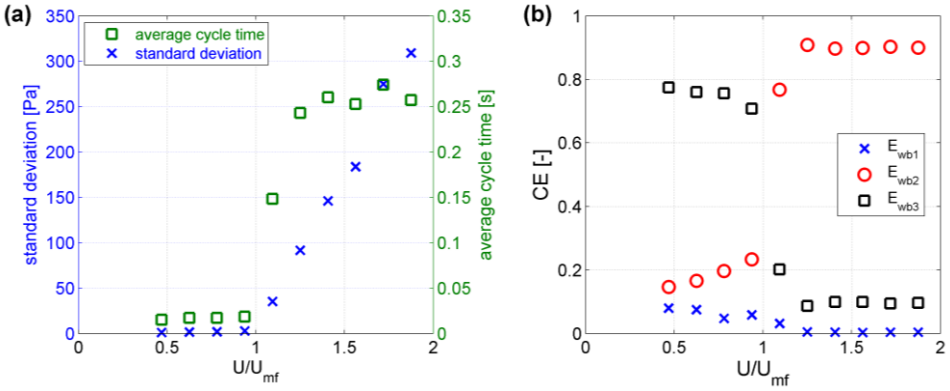

Fig. 2. Behavior of the control variables versus the air flow ratio. (a) Standard deviation and average cycle time. (b) Energy distributions.

Frequency domain analysis

The energy contained within the power spectrum of the pressure signal can be used as a variable to monitor the fluidization behavior (9). The ratio between the energy in a region and the total energy of the power spectrum is called wide band energy. In order to estimate properly the wide band energy it is necessary to divide the energy distribution into three regions within the frequency domain. Analyzing the cumulative energy distribution of the bed under nominal conditions, the frequency domain presents a first region, E_{wb1}, ($\Delta f \leq f \leq 1.3$ Hz) with less than 0.2% of the total energy (5). That frequency energy region is related to the bubble dynamics (9). The second region, E_{wb2}, contains the 90% of the energy of the signal and was defined from 1.3 Hz to 4.5 Hz, in which the dominant frequencies are codified, representing the bulk movement of the bed (9). Finally, the third region, E_{wb3}, covered from 4.5 Hz to the Nyquist frequency (200 Hz) with almost the 10% of the energy. It identifies the finer structures that are not predominantly governed by the bulk movement of the flow.

The increase of the air flow produced a clear change on all energy distributions, Fig. 2-b.

RESULTS AND DISCUSSION

The results show the application of the proposed methodology to the fluidized bed control. First the fluidized bed was studied at nominal conditions with a static distributor for 30 minutes. Once the control chart was designed, several tests of agglomeration were carried out to see the dynamic response of the control charts.

Implementation of the moving mean chart

In the basic design of a moving mean control chart, the sample size of the moving window (W_t) used to draw the control charts must be specified. The length of the sample size is restricted by two limits. The first limit is referred to the minimum size of the moving window, which is related to the dynamic of the fluidized bed. According to Wilkinson (10), a time length of W_t = 25 seconds can be considered a reasonable minimum time length to satisfy the objective of a reliable measurement for the standard deviation.

The second limit is related to the statistical basis of the moving mean control charts. In general, when the subgroup size is increased, the control limits are closer to the mean value and, as a consequence, the detection of small variations outside of the thresholds is easier. However, a drawback of increasing the sample size (W_t) is the time lag in following any trend, because of the averaging effect produced by the increase of the number of points used to estimate the control variable. This averaging effect was studied comparing three different window lengths of 25, 50 and 100 s. The time at which the control variables exceeded the control thresholds was analyzed when there was an abrupt change on the fluidization quality. That change was achieved through the punctual injection of 150 ml of water to the surface of the bed. As expected, the control variables presented an increase of around 10% to 60% in the time needed to detect the leave of the control thresholds as the window length increases. Thus, the moving window size was fixed to the value of 25 s since it satisfies both limits, which were referred to the minimum size of the moving window or to the time lag of the moving mean control charts.

A fundamental assumption in the development of the control chart is that the underlying distribution of the control variable is normal. However, it is necessary to check this hypothesis in order to estimate the correct control limits. The values of the kurtosis (k) and the skewness (s) for each variable, which are presented in Table 1, are sligthly deviatied from the normal values of k = 3 and s = 0. Therefore, the underlying distributions of the controlled variables were searched applying the Kolmogorov-Smirnov test, Eq (1), to the normal, gamma and weibull distributions (11).

$$D = \sup_x \left| F_x(x) - F(x) \right| \tag{1}$$

Table 1. Kurtosis and skewness values for the variables histograms.

	σ	*tav*	E_{wb1}	E_{wb2}	E_{wb3}
Kurtosis (k)	2.64	2.72	3.41	3.59	3.53
Skewness (s)	-0.30	-0.29	0.50	-0.72	0.72

The Figure 3 presents the evolution of the Kolmogorov-Smirnov test versus the signal length analyzed. The distribution is selected when this test reaches a minimum value. For the first 10 minutes, Fig. 3 showed that the experimental distribution can be adjusted to any theoretical distribution considered, since all the experimental histograms presented bell-shape distributions. In such a zone, the small number of points available for the distribution estimation make possible to fit the experimental values with any of the theoretical distributions considered. As the number of measurements increase, the theoretical distribution that fits the observed values is obtained. Therefore, there was a minimum time of the signal length at which the experimental distribution can be described only by one theoretical distribution. This time was fixed when the Kolmogorv-Smirnov statistic reached a constant trend (Fig. 3-a/c/e) or when it started a downward trend (Fig. 3-b/d). The normal distribution can describe the standard deviation and the average cycle time (Fig. 3-a/b), whereas the gamma distribution will describe the energy distributions of Regions I and III (Fig. 3-c/e). The energy of the Region II will be approximated by the weibull statistic (Fig.3-d).

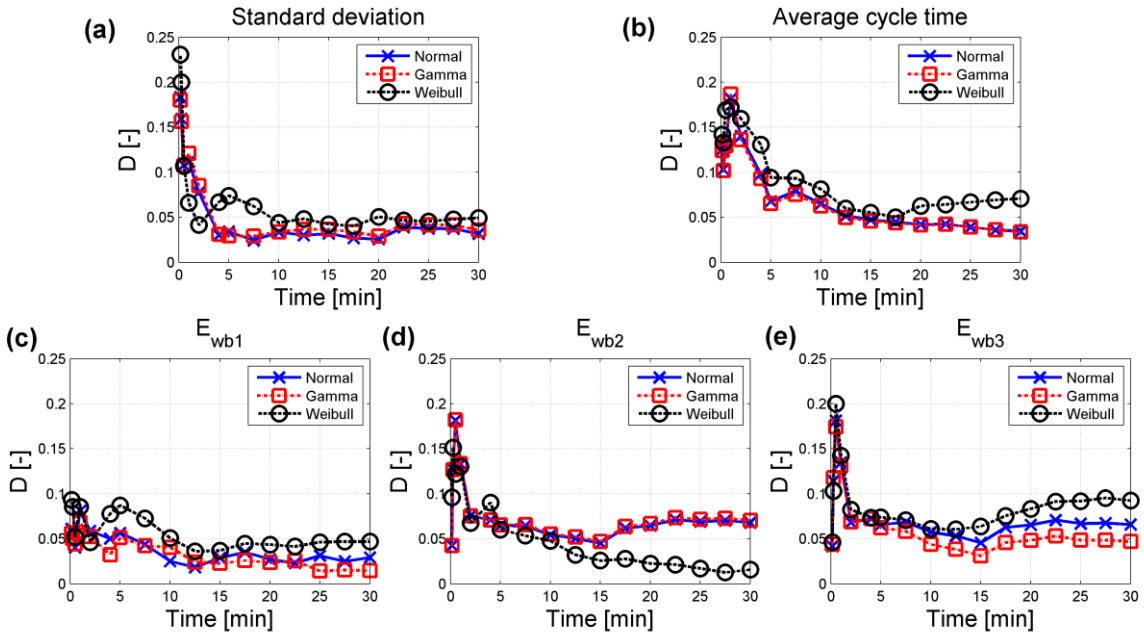

Fig. 3. Kolmogorov-Smirnov statistic as a function of the signal length. (a) Standard deviation. (b) Average cycle time. (c) Wide band energy I. (d) Wide band energy II. (e) Wide band energy III.

SPC applied to agglomeration phenomena

The results for the water injection are presented in Figs. 4 and 5, where the control strategy proposed was applied to the control variables for two types of recuperation, i) applying the rotating distributor when the bed is defluidized, and ii) 'auto-recuperation' with the static distributor. The control thresholds were estimated using the statistical distributions obtained before. The upper and lower action lines (*LAL* and *UAL*) were estimated assuming the 0.001 probability of exceeds these limits in one direction, whereas the lower and upper warning limits (*LWL* and *UWL*) were estimated for the 0.025 probability.

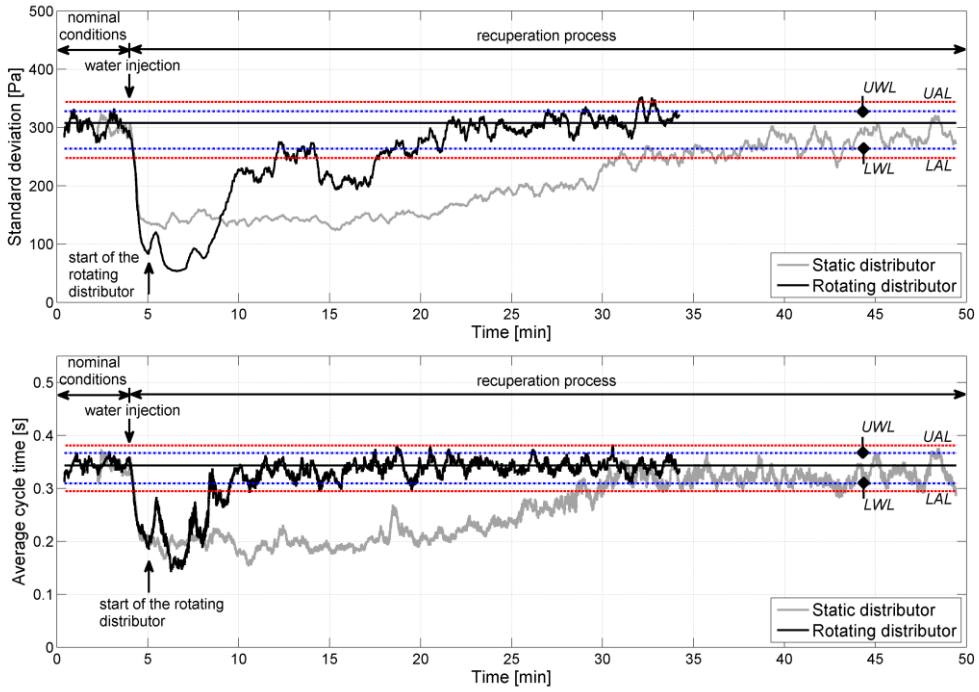

Fig. 4. Punctual injection of 150 ml of water, time domain analysis. (a) Standard deviation control chart. (b) Average cycle time control chart.

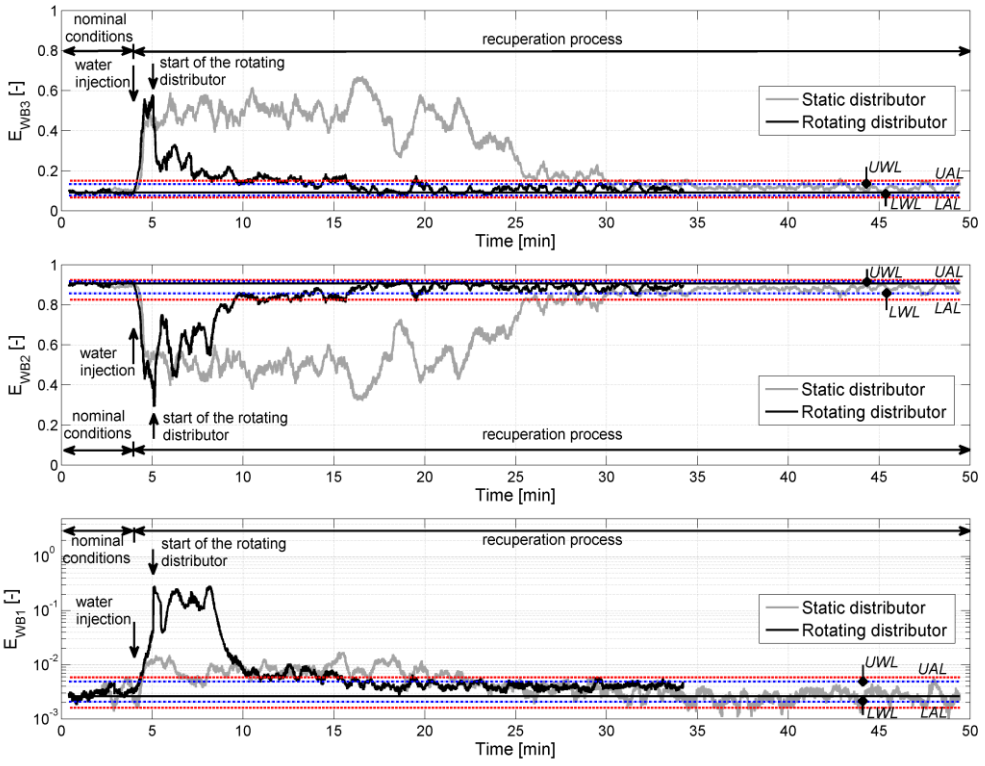

Fig. 5. Wide band energy control charts for the punctual injection of 150 ml of water. (a) Region III, E_{wb3}. (b) Region II, E_{wb2}. (c) Region I, E_{wb1}.

As it can be seen in Figs. 4 and 5, the control variables show a clear influence of the punctual water injection on the fluidization quality. During the first 4 minutes the bed was operated between the warning control limits until the water injection. In both tests, the agglomerates formation caused an abrupt decrease of the standard deviation, which fell from the control state to the out of the control state with a value below the lower action line (*LAL*) in around 15 s for all the variables (Figs. 4 and 5). The agglomerates tend to settle on top of the distributor near the injection zone causing the appearance of channels. Focusing on the static distributor test, these channels were detected by the high values of the energy distribution of Region III (Fig. 5-a). However, the energy of Region II, which represents the bulk movement of the bed, was out of the control state for 25 minutes showing that the bed was completely defluidized after the injection of water. Similar time is needed to recover the fluidization quality for the average cycle time (Fig. 4-b), and for the energy of Region III (Fig. 4-a). The energy of Region I was recovered 18 minutes after the punctual injection, showing that the bubbling pattern was recuperated before the other phenomenon. In contrast, the standard deviation was out of control for 35 minutes. Such high recovery times can be explained since the agglomerate breakage was a slow phenomenon in the static distributor test because the drying mechanisms of the particles were controlled by the slow diffusion velocity of the water inside of the bed (12).

In the second run the rotating distributor was started 1 minute after the water injection. This induced the breakage of the agglomerates placed on top of the distributor, since the dead zones between the holes of the distributor were broken improving the radial and axial mixing at the bottom of the bed (13). The breakage of the channels was immediately detected by the energy of the Region III (Fig. 5-a), whose energy was transferred to the low frequency region (Fig. 5-c) reaching values higher than the previous showed when the bed was not fluidized (Fig. 2). Once the agglomerates were eroded, the energy distributions recovered the control state at the same time 11 minutes after the start of the distributor motion. However, the average cycle time (Fig. 4-b) recovered the control state only 6 minutes after the starting of the distributor rotation, indicating the bubble eruption in the bed. It is worth to point out that, at that time (6 minutes after the start of the distributor motion), all the variables were near to the *LAL* threshold. The standard deviation (Fig. 4-a) presented some fluctuations around the *LAL* threshold pointing the variations produced in the fluidization behavior caused by the agglomerates breakage. In that case, the recuperation time was 16 minutes.

CONCLUSIONS

The proposed methodology shows its capability to detect the defluidization of the bed, the formation of the channels, and its latter disappearance by the drying effect of the air flow or by the breakage effect of the rotating distributor. It was shown that there was a minimum signal length needed to statistically describe these control variables.

ACKNOWLEDGMENTS

The author would like to thank the financial support from Project DPI2009-10518 (MICINN).

NOTATION

Symbols			Subscripts	
h_b	fixed bed heigth	m	*1,2 ,3*	frequency regions
D	Kolmogorov-Srminov statistic	-	*mf*	minimum fluidization
E_{wb}	wide band energy	-	*r*	rotating distributor
k	kurtosis	-	*s*	static distributor
s	skewness	-	**Abbreviations**	
tav	average cycle time	s	*BFB*	bubbling fluidized bed
U	superficial velocity	m/s	*LAL*	lower action line
W_t	window length	s	*LWL*	lower warning line
			SPC	statistical process control
Greek letters			*UAL*	upper action line
σ	standard deviation	Pa	*UWL*	upper warning line

REFERENCES

(1) C.A.M. Silva, M.R. Parise, F.V. Silva, O.P. Taranto. Control of fluidized bed coating particles using Gaussian spectral pressure distribution, Powder Technol., 212(3), 445-458, 2011.

(2) W.A. Shewhart. Economic quality control of manufactured product. Bell System Technical Journal, 9(2), 1930.

(3) D. Geldart. Types of Gas Fluidization. Powder Technol, 7(5), 285-292, 1973.

(4) J.R. van Ommen, J.C. Schouten, M.L.M. vander Stappen, C.M. van den Bleek. Response characteristics of probe-transducer systems for pressure measurements in gas-solid fluidized beds: how to prevent pitfalls in dynamic pressure measurements. Powder Technol, 106(3), 199-218, 1999.

(5) J. Gómez-Hernández, A. Soria-Verdugo, J.V. Briongos, D. Santana. Fluidized bed with a rotating distributor operated under defluidization conditions. Chem.Eng.J., 195–196(0), 198-207, 2012.

(6) C. Sobrino, J.A. Almendros-Ibanez, D. Santana, M. De Vega. Fluidization of Group B particles with a rotating distributor. Powder Technol, 181(3), 273-280, 2008.

(7) J.R. van Ommen, S. Sasic, J. van der Schaaf, S. Gheorghiu, F. Johnsson, M. Coppens. Time-series analysis of pressure fluctuations in gas-solid fluidized beds - A review. Int. J. Multiphase Flow, 37(5), 403-428, 2011.

(8) M.L.M. vander Stappen. Chaotic hydrodynamics of fluidized beds. PhD thesis, Delft University of Technology, The Netherlands, 1996.

(9) F. Johnsson, R.C. Zijerveld, J.C. Schouten, C.M. van den Bleek, B. Leckner. Characterization of fluidization regimes by time-series analysis of pressure fluctuations. Int.J.Multiphase Flow, 26(4), 663-715, 2000.

(10) D. Wilkinson. Determination of Minimum Fluidization Velocity by Pressure Fluctuation Measurement. Can.J.Chem.Eng., 73(4), 562-565, 1995.

(11) R.B. D'Agostino, M.A. Stephens. Goodness-of-fit techniques. Marcel Dekkel, 1986.

(12) S. Weber, C. Briens, F. Berruti, E. Chan, M. Gray. Agglomerate stability in fluidized beds of glass beads and silica sand. Powder Technol, 165(3), 115-127, 2006.

(13) A. Soria-Verdugo, N. Garcia-Hernando, J.A. Almendros-Ibanez, U. Ruiz-Rivas. Motion of a large object in a bubbling fluidized bed with a rotating distributor. Chem.Eng.Process, 50(8), 859-868, 2011.